

THE SPECTRUM OF THE BLACK HOLE X-RAY NOVA V404 CYGNI IN QUIESCENCE AS MEASURED BY *XMM-NEWTON*

CHARLES K. BRADLEY¹, ROBERT I. HYNES¹, ALBERT K. H. KONG², C. A. HASWELL³, J. CASARES⁴, E. GALLO⁵
Draft version November 6, 2018

ABSTRACT

We present *XMM-Newton* observations of the black hole X-ray nova V404 Cyg in quiescence. Its quiescent spectrum can be best fitted by a simple power-law with slope $\Gamma \sim 2$. The spectra are consistent with that expected for the advection-dominated accretion flow (ADAF). V404 Cyg was roughly equal in luminosity compared to the previous observation of *Chandra*. We see variability of a factor of 4 during the observation. We find no evidence for the presence of fluorescent or H-like/He-like iron emission, with upper limits of 52 eV and 110 eV respectively. The limit on the fluorescent emission is improved by a factor of 15 over the previous estimate, and the restriction on H-like/He-like emission is lower than predicted from models by a factor of roughly 2.

Subject headings: binaries: close — black hole physics — stars: individual (V404 Cyg) — X-rays: stars

1. INTRODUCTION

Low Mass X-ray Binaries (LMXB) are binary systems with a black hole or neutron star primary and usually a late-type main sequence or evolved donor star (Remillard & McClintock 2006). The donor is filling its Roche Lobe and therefore transfers mass to the primary component via an accretion disk. This material within the disk emits light at all wavelengths, but is generally very faint while in quiescence, however it can become very bright in X-rays and highly variable during rare outbursts, making these objects very interesting for study in the area of accretion physics. X-ray observations of these objects only tell a portion of the story, as their orbital periods and masses are determined by optical observation of their counterparts. These orbital periods typically range from tens of minutes to days.

Several sources of quiescent X-ray emission have been discussed for black hole X-ray binaries (BHXBs). It has been suggested that advection-dominated accretion flows (ADAF) can explain the optical and X-ray emission and the X-ray spectra seen in quiescence (see, e.g., Narayan et al. 2002). V404 Cyg has been used as the primary testbed for many of these models because of its accessibility with X-ray observatories. These flows also provide a natural explanation for the luminosity difference between black hole and neutron star systems (Garcia et al. 2001). The radiatively inefficient accreting material must impact the surface of a neutron star and be reprocessed, whereas in the black hole case, it simply disappears beyond the event horizon. It has also been proposed by Fender, Gallo, & Jonker (2003) that the system could go into a “jet-dominated” state at such low accretion rates

where a majority of the energy is released in the outflow instead of the ADAF. It has also been suggested that emission from a disk plus an optically thin corona could explain the quiescent emission and that the standard disk + corona model should not be discarded outright (Nayakshin & Svensson 2001). A hybrid jet/ADAF model has been suggested by Yuan et al. (2005) applied to XTE J1118+480 that accounts for the spectral and timing features of that system. A similar model by Malzac et al. (2004) to the same system has also been proposed that reproduces the timing features.

V404 Cyg was originally discovered by *Ginga* during outburst in May 1989 (Makino et al 1989). Optical observation of V404 Cyg determined a mass function of $f(M) = 6.08 \pm 0.06 M_{\odot}$ (Casares & Charles 1994, Casares, Charles, & Naylor 1992) and an orbital period of 6.47d. Combined with limits on the inclination ($i = 56^{\circ}$) we deduce a black hole mass of approximately $12 M_{\odot}$ (Shahbaz et al. 1994), orbited by a K0IV star of $\sim 0.7 M_{\odot}$. Of the stellar-mass black hole population, V404 Cyg is the X-ray brightest and most accessible object in quiescence. V404 Cyg is known to vary in X-rays (Wagner et al. 1994, Kong et al. 2002) by a factor of 2 in a timescale of just 30 minutes, and by a factor of 10 within 12 hours in quiescence.

The origin of the quiescent variability remains uncertain, however, with possibilities ranging from magnetic reconnection events, to local changes in the accretion rate. Optical and X-ray variations in V404 Cyg in quiescence have been shown to be fairly well correlated by Hynes et al. (2004). They showed that variability is mirrored well by H α and to a lesser extent by the optical continuum. This correlated variability, generally attributed to irradiation of the outer cool(er) disk, is commonly seen in bright X-ray states for both neutron star and black hole systems (Hynes 2005).

Here we report the analysis of *XMM-Newton* spectra of the brightest quiescent BHXB observed, V404 Cyg. This is the highest quality X-ray spectrum of a quiescent BHXB yet obtained. We briefly describe previous quiescent observations of this source in §2. In §3 we outline the analysis procedure and report results in §4 and §5.

¹ Department of Physics and Astronomy, Louisiana State University, Baton Rouge, LA, 70803

² Kavli Institute for Astrophysics and Space Research, Massachusetts Institute of Technology, 77 Massachusetts Avenue, Cambridge, MA, 02139

³ The Open University, Walton Hall, Milton Keynes, MK7 6AA, UK

⁴ Insitute de Astrofísica de Canarias, Via Lactea, 38200 La Laguna, Tenerife, Spain

⁵ University of California, Santa Barbara, CA, 93106

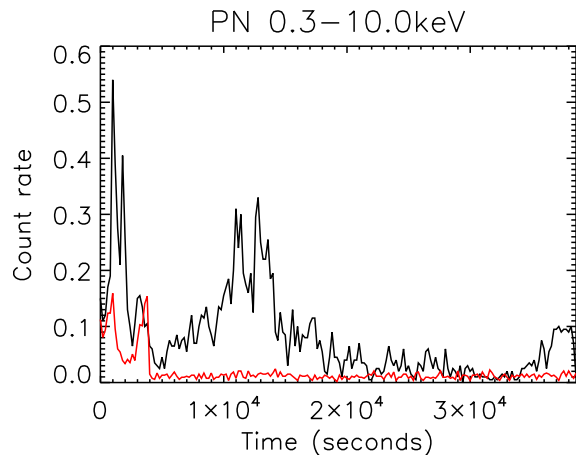


FIG. 1.— PN camera lightcurve, source and background, binned at 200s

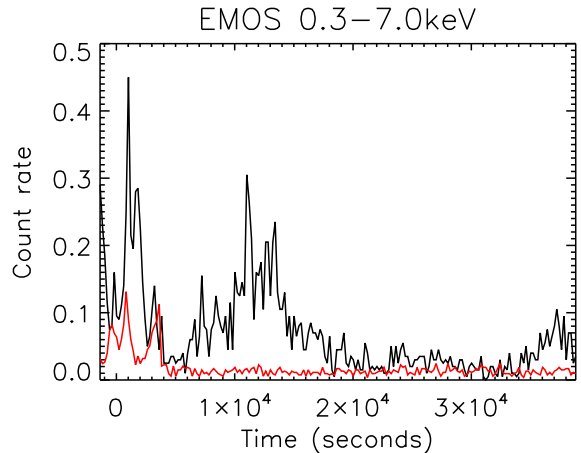


FIG. 2.— Summed EMOS lightcurves with background, binned at 200s

They are then discussed in § 6.

2. PREVIOUS OBSERVATIONS OF V404 CYG

This bright quiescent BHXB has been observed by *ROSAT*, *ASCA*, *BEPP0-SAX*, and twice by *Chandra*. In general, its spectrum has been well fitted by a simple power-law model with photon index $\Gamma \sim 2$ with varying estimates of N_{H} in the range $\sim 0.7 - 2.3 \times 10^{22} \text{ cm}^{-2}$ and a luminosity of $\sim 1.0 \times 10^{33} \text{ erg/s}$ (see Table 1; Narayan et al. 1997, Kong et al. 2002). Early estimates of the spectrum were consistent with those derived by *Chandra*, when one considers that the *ROSAT* data are based on energies below 2.5 keV in which range errors on N_{H} and Γ are strongly positively correlated. Previous upper limits on the equivalent width of the 6.4 keV iron line emission were found to be $\sim 800 \text{ eV}$ (Kong et al. 2002) and were too high to constrain spectral models that included line emission.

3. XMM OBSERVATIONS AND DATA REDUCTION

V404 Cyg was observed by *XMM-Newton* on 2005 November 8-9. The observation lasted 40ks. The three EPIC cameras were all active during the observation: pn, EMOS1, and EMOS2. The three cameras were operated with a medium filter in Imaging Full Window Mode. Total background corrected counts from the three cameras are given in Table 2. For this paper we analyzed standard pipeline-processed event files with SAS v6.2.0. In order to study the temporal behavior of V404 Cyg we accumulated its pn lightcurve in the energy range 0.3-10 keV, using an extraction radius of 6 pixels (Figures 1-2). EMOS camera analysis is restricted to the 0.3-7 keV range, also with an extraction radius of 6 pixels. Corresponding backgrounds were taken from the same chip as the source but far enough away from it so as to not be affected by the wings of the point spread function, with an extraction radius of 16 pixels in pn and in MOS. These lightcurves show variability of a factor of 4 in count rate within 10ks, and a large amplitude flare is detected at the very beginning of the run with a duration of about thirty minutes.

The pn pixels are larger than the EMOS, so no multi-pixel events are expected by the soft-proton background,

therefore a standard Pattern 0 cleaning was used for the lightcurve. Standard pn filtering was accomplished with XMMEA-EP and EMOS filtering with XMMEA-EM. We measured a source count rate of 0.035 s^{-1} for pn and an average of 0.012 s^{-1} each for the two EMOS.

4. CONTINUUM SPECTRAL ANALYSIS

Spectra were extracted with XMMselect and were analyzed with XSPEC v12.2⁶ and we report those results here. Spectral extraction was done with XMMEA-EP and Pattern 4. EMOS extraction was done likewise with XMMEA-EM and with Pattern 12. Bin sizes in extraction were 5 counts/channel for pn and 15 for the EMOS cameras, as suggested in the *XMM-Newton* Users Guide⁷ for optimal use of the standard response matrices. Single and double events were included under a Pattern 4 extraction for pn, and all valid patterns were kept for EMOS. Response files were made using standard SAS tools to check against the standard version, with consistent results for the spectral fits from both. Further spectral analysis was done between 0.3-10 keV for pn and 0.3-7 keV with MOS.

We have chosen to use χ^2 Churazov-weighted statistics (Churazov 1996) in our analysis, since we feel these to be more applicable when line diagnostics are to be done. CASH statistics (Cash 1979) were used as a check. For this we used lightly binned data (5cts/bin) for χ^2 statistical fits. We then fit the data with many single-component spectral models such as power-law, thermal bremsstrahlung, Raymond-Smith (1977), and blackbody, including interstellar absorption. A broken power-law model was also tried with data from the onboard pn camera, but fits were poor to EMOS1 and EMOS2 data. Fits to many other single and multiple component models within XSPEC were tried (comptonized blackbody, blackbody with power-law, etc.), but in those cases the error bars on fitted parameters were unreasonably large or the fit was too poor. The best-fit parameters for each of the three cameras used, by both CASH and χ^2 statistics, are consistent between the two fitting methods and only χ^2 results are reported herein. The quoted errors

⁶ <http://heasarc.gsfc.nasa.gov/docs/xanadu/xspec/index.html>

⁷ http://xmm.esac.esa.int/external/xmm_user_support/documentation/sas_us

TABLE 1
PREVIOUS QUIESCENT OBSERVATIONS

Source	Date	Instrument	N_H (10^{22} cm^{-2})	Γ	Luminosity ($10^{33} \text{ erg s}^{-1}$)	Distance (kpc)	References
V404 Cyg	1992 Nov	<i>ROSAT</i>	2.29 ^a	6 ^a	8.1 (0.1–2.4keV)	3.5	1
			2.1 ^a	$4.0^{+1.9}_{-1.5}$	1.1 (0.7–2.4 keV)		2
	1994 May	<i>ASCA</i>	$1.1^{+0.3}_{-0.4}$	$2.1^{+0.3}_{-0.3}$	1.20 (1–10 keV)		3
	1996 Sept	<i>BeppoSAX</i>	1.0 (fixed)	$1.9^{+0.6}_{-0.3}$	1.04 (1–10keV)		4
	2000 Apr	<i>Chandra</i>	0.69 ± 0.08	1.81 ± 0.14	2.07 (0.3–7keV)	3.5	5
	2003 Jul	<i>Chandra</i>	0.75 ± 0.07	$2.17^{+0.11}_{-0.15}$	1.10 (0.3–7keV)	3.5	6
	2006 Nov	<i>XMM-Newton</i>	0.88 ± 0.6	2.09 ± 0.08	1.07 (0.3–10keV)	3.5	7

NOTE. — (1) Wagner et al. 1994; (2) Narayan et al. 1996; (3) Narayan et al. 1997a; (4) Campana et al. 2001; (5) Kong et al. 2002; (6) Hynes et al. (in prep), (7) this result

^adenotes that uncertainty was not given

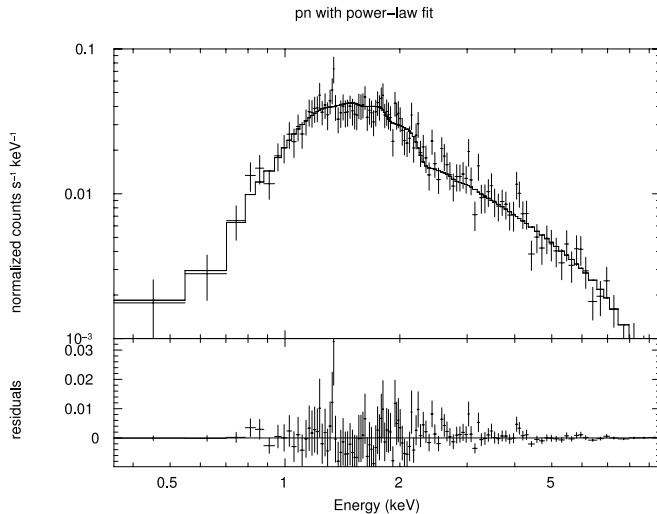


FIG. 3.— Comparison of the PN spectrum with the best-fit power-law model. In the lower panel the residuals between data and model are shown, binned for visual clarity

on the derived model parameters correspond to a 90% confidence level.

Only two of the models reported give statistically acceptable fits to the data ($\chi^2/\nu \lesssim 1$). The power-law model provides the best fit to the data, and yields parameters consistent with previous observations (e.g. $\Gamma \sim 2.0$; see Table 2), and was then used for line diagnostics. Bremsstrahlung is also acceptable, while Raymond-Smith and blackbody model fits are rejected. This best fitting model is shown in Figures 3 and 4.

The pn and EMOS spectra give consistent fit parameters with quoted uncertainties (see Table 2). Combined data fits restrict $\Gamma \sim 2.09$, $N_H = 0.7 - 0.9 \cdot 10^{22} \text{ cm}^{-2}$ for the two models considered, but with a luminosity for the two of $L_x \sim 1.0 \times 10^{33} \text{ erg s}^{-1}$, consistent with previous results. In the following analysis, we aim to constrain the possible presence of the iron line and consider only the pn spectra, due to the higher statistics at high energies.

5. LINE DIAGNOSTICS

5.1. Iron $K\alpha$ lines in XRBs

Iron $K\alpha$ emission features have been detected in other X-ray binaries before, usually but not exclusively (Oosterbroek et al. 2001) in BH transients. A few recent examples of stellar-mass BH cases are XTE J1650-500 (Miller et al. 2002), SAX J1711.6-3808 (In’t Zand et

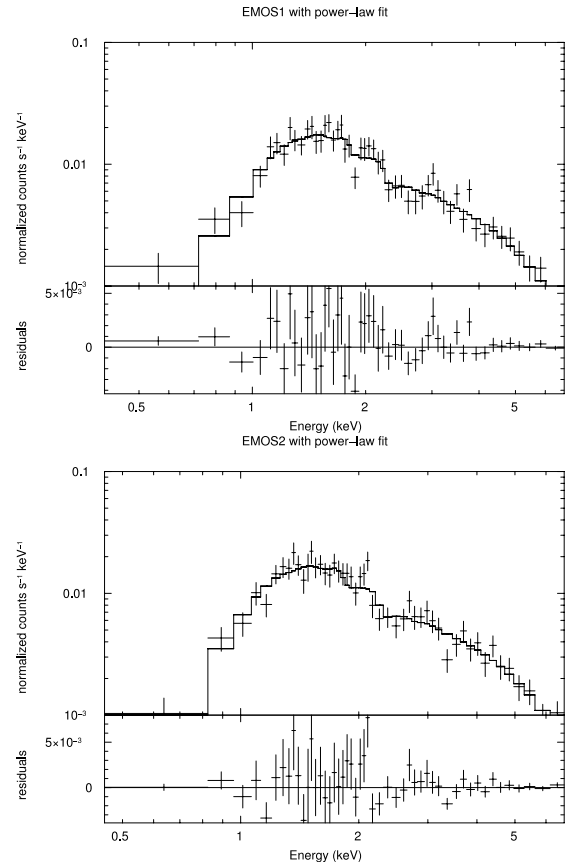


FIG. 4.— EMOS 1 and 2 spectrum, 0.3–7 keV, fitted with the power-law model and showing residuals, binned for visual clarity

al. 2002b), XTE J2012+381 (Campana et al. 2002) and GRS 1915+105 (Martocchia et al. 2002). However these detections are generally weak or broad lines. See also Miller (2006) for a recent review.

Before searching for an iron $K\alpha$ line in our data, it must be stressed that detection of broad lines represents an observational challenge, due to limited statistics and uncertainty in the shape of the underlying continuum. The lines are easier to detect if the disk is truncated at larger radii and/or the radial emissivity profile is not centrally concentrated, so that the line is not broad and can be distinguished from the continuum. On the other hand, if the black hole is rapidly spinning so that a standard cold

TABLE 2
BEST-FIT PARAMETERS FOR POWER-LAW AND BREMSSTRAHLUNG MODELS

Instrument	Model	N_H (10^{22} cm^{-2})	Photon Index	kT	Normalization at 1 keV ($\text{ph keV}^{-1} \text{ cm}^{-2} \text{ s}^{-1}$)	χ^2_ν/dof	f_X (0.3–10keV) ^a ($\text{erg cm}^{-2} \text{ s}^{-1}$)	counts
pn	PL	0.86 ± 0.7	2.10 ± 0.10	–	$(1.98 \pm 0.2) \times 10^{-4}$	0.75/115	1.04×10^{-12}	1404
	bremsstrahlung	$0.69^{+0.05}_{-0.02}$	–	$4.88^{+0.73}_{-0.6}$	$(1.67 \pm 0.2) \times 10^{-4}$	0.77/115	7.47×10^{-13}	
EMOS1	PL	0.859 ± 1.2	2.04 ± 0.18	–	$(1.99 \pm 0.4) \times 10^{-4}$	0.96/48	1.06×10^{-12}	497
	bremsstrahlung	$0.67^{+0.1}_{-0.08}$	–	$5.40^{+1.9}_{-1.25}$	$(1.72 \pm 0.2) \times 10^{-4}$	1.01/48	7.31×10^{-13}	
EMOS2	PL	0.927 ± 1.3	2.06 ± 0.18	–	$(2.07 \pm 0.4) \times 10^{-4}$	0.92/47	1.12×10^{-12}	519
	bremsstrahlung	$0.75^{+0.1}_{-0.09}$	–	$4.91^{+1.72}_{-1.09}$	$(1.80 \pm 0.3) \times 10^{-4}$	1.05/47	7.37×10^{-13}	
JOINT FIT	PL	0.88 ± 0.6	2.09 ± 0.08	–	$(2.02 \pm 0.2) \times 10^{-4}$	0.86/216	1.08×10^{-12}	
	bremsstrahlung	0.70 ± 0.4	–	$4.93^{+0.59}_{-0.49}$	$(1.72 \pm 0.1) \times 10^{-4}$	0.89/216	7.81×10^{-13}	

NOTE. — Errors are at 90% c.l. for a single interesting parameter;
^aunabsorbed flux; flux is in 0.3-7 keV range for MOS

disk can extend to small radii and the profile is centrally concentrated (as it should be), the line becomes so broad that its low contrast against the continuum makes it a challenge for detection even for *XMM-Newton* (Fabian & Miniutti 2005). In the latter case, the line would only be detected easily if the system has a super-solar abundance and/or a large reflective component. Fortunately, in quiescence the disk is not expected to extend close to the black hole, and thus we do not expect a broad line, at least in the dominant paradigm of an evaporated inner disk. While, Nayakshin & Svensson (2001) dispute that the disk truncates in this way, they also do not expect central concentration of the X-ray emitting region. In their model, most of the X-ray emission comes from a corona above a thin disk at large radii; hence a narrow line would again be expected. Given the limited statistical quality of our data, we therefore confine our search to narrow lines. We should keep in mind, however, that if the line were much broader than these expectations then we are unlikely to detect it without a much higher quality spectrum and coverage of the high energy continuum.

5.2. Observational constraints on V404 Cygni

Our spectral analysis of V404 Cyg shows no evidence for a narrow 6.4 keV iron line. From adding a gaussian component to the best-fitting model, (fixed width 0.1 keV, corresponding to instrumental resolution) we establish an upper limit of ~ 52 eV for this line (90 % confidence), well below all previous estimates (~ 800 eV, Kong et al. 2002). We then repeated this analysis using CASH statistics, and find the results to be consistent.

Prompted by predictions of emission in ADAF-like flows by Narayan & Raymond (1999), we then test-fitted a 6.7 keV gaussian (from He-like Fe XXV) to the spectrum, and detect no significant emission there either with an upper limit of ~ 110 eV (0.1 keV fixed width; 90 % confidence) on the feature. The total group of Fe line widths in their paper sums to roughly 230 eV, a factor of about 2 above our results. A close-up of the 5-10 keV region of the spectrum is presented in Fig. 5.

There are some features seen in the spectrum of V404 Cyg and possibly within previous results (Hynes et. al in prep) that may indicate the presence of line emission at just above 4 keV. This line corresponds to a line predicted from Ca XIX/XX in Narayan & Raymond (1999). We again added in a gaussian line component (allowing the energy to vary) to the power-law fit at an energy of 4.08

keV (Ca XX Ly α), and find a fitted equivalent width of ~ 117 eV, well above the 2.7 eV equivalent width predicted in their paper, for a model with wind outflows. The 90% confidence range on the equivalent width is from 4.0-210 eV.

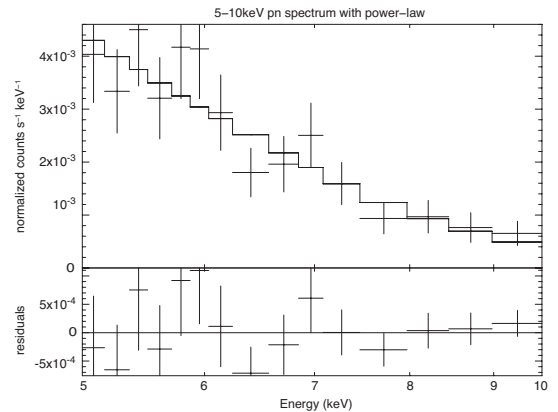


FIG. 5.— pn spectrum in energy range of 5-10 keV, with powerlaw model overlaid

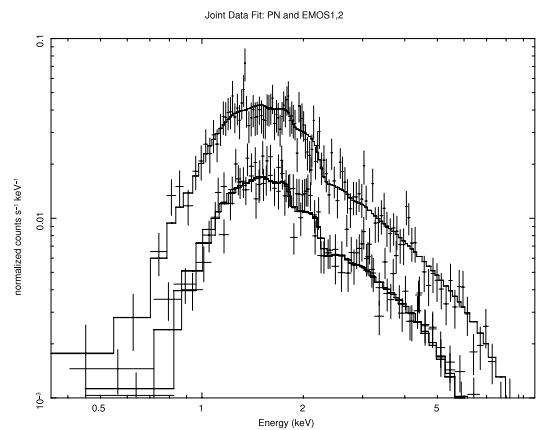


FIG. 6.— pn and EMOS spectra joint fit to power-law model

6.1. Iron fluorescent emission

One would expect 6.4 keV fluorescent emission from the presence of cold material near the X-ray emitting region, or an extended emission region above the disk that illuminates cold material below. For typical inclination angles, (e.g., $i = 56^\circ$ for V404 Cyg) the absence of such a feature constrains the reflection fraction and suggests that there is no cold matter near the X-ray emission region, or at least that such material does not subtend a large solid angle as seen by the X-ray source. George and Fabian (1991) considered a model in which the X-ray source was located at a height above the central region of a standard disk, for a semi-isotropically and isotropically illuminated cold slab (without rotation), and calculated equivalent widths of the $K\alpha$ line for varying inclinations (relative to the observer) and incident power-law indices. Their predicted equivalent width for the power-law index and inclination ($i = 56^\circ$) of V404 Cyg for the 6.4 keV feature was $\sim 110 - 120$ eV, a factor of 2 higher than our upper limit (see Figure 14 of their paper). The lack of the a narrow 6.4 keV line is then inconsistent with the simplest geometry of an X-ray source sandwiching a cold, slowly rotating slab. In particular our observations would seem to disagree with expectations of the Nayakshin & Svensson model (2001) for this system because their emission comes from large radii, where there should be a cold thin disk, so we would expect a narrow line to be present. The Nayakshin & Svensson model has other difficulties as well, such as higher luminosity predictions than what are observed for quiescent BH systems. At these luminosities we would expect some signature of 6.4 keV emission.

The discussion above has, of course, neglected rotation. The 0.1 keV fixed width adopted above corresponds to an unresolved line from a region extending no closer than $\sim 1000_{\text{sch}}$ to the compact object. This is smaller than typically assumed in modeling advective flows, but we cannot observationally exclude the possibility of broad line emission from a region closer to the black hole.

6.2. 6.7 keV emission

We would expect Fe XXV $K\alpha$ emission at an energy of 6.7 keV from a hot coronal/ADAF flow with high collisional rates. The lack of any such 6.7 keV line emission may point back to earlier ADAF models of Comptonized thermal synchrotron emission within a small region close to the black hole. Such a small emitting region would also fail to properly illuminate the disk surface to achieve significant 6.4 keV emission.

In particular, one of the ADAF models with moderately strong outflows presented in Narayan & Raymond (1999) is ruled out. This paper specifically addresses X-ray spectra of systems thought to contain an ADAF flow. Their spectral model consisted of what is basically a Raymond-Smith (1977) plasma with an additional Compton component added in. They follow a method outlined in Quataert & Narayan (1999), and assign reasonable values to the microscopic parameters of the system, specifically the viscosity parameter and plasma parameter, which seem to reproduce the correct spectral index otherwise, and vary the fraction of dissipated heat that goes directly into the electrons between their wind and no-wind models. The spectral calculation starts at a

radius of 100 Schwarzschild radii and proceeds outward, with the intent to target the transition region from standard thin disk to ADAF where most of these lines would originate. They do not include synchrotron emission or the effects of Comptonization, and no Doppler smearing, assumed to be small at the radii of interest. Inner regions are assumed to be so hot that the gas is completely ionized, and here they computed the continuum emission but no line emission.

In this paper it was suggested by the authors that the equivalent width of lines correspond to the size of the ADAF region, and that for a given size the widths increase with outflow strength. Lower accretion rates would lead to increased bremsstrahlung emission, and equivalent widths increase. A bremsstrahlung model fit to the data is statistically acceptable, but we see no lines, the most prominent of which should have been at 6.7 keV. Based on their conclusions, our results would indicate that V404 Cyg is a Compton-dominated system with a weak outflow, if one is present. However the assumptions made and outlined above may be called into question. The plasma parameter, the viscosity, the accretion rate's dependence on radius, or the fraction of heat transferred to the electrons in the ADAF could all very well be different from that assumed. They state that their model is insensitive to the values assumed for the viscosity and plasma parameters however. Their model assumes ionization equilibrium, but they point out that departure from this will only make the line intensities larger which is in the opposite sense to that caused by photoionization. The modeling of the corona above the outer thin disk is crude, however. The strongest X-ray line emission occurs for $T_e \sim 10^7 - 10^8$ K, suggesting that the source of the X-ray emission is above this temperature.

A simpler model of hot optically-thin plasma emission in ionization equilibrium (Raymond & Smith 1977) appears to be statistically ruled out by the combination of our results with those previously published (Kong et al. 2002).

6.3. Other explanations for the absence of line emission

Absence of any iron line may indicate that the system is underabundant in iron, all the material present in the X-ray emitting region is completely ionized, or perhaps that resonant trapping is efficiently eliminating any line emission (Matt et al. 1993, 1996). A hole in the disk filled with an ADAF would explain the absence of cold material, but we may still expect reflection. The presence of a central ADAF should diminish the strength of any reflective feature (Gierlinski et al. 1997) but not necessarily push it to zero (Miller et al. 2002).

The absence of any Fe line is not likely to be caused by underabundance because a strong Fe line feature with an equivalent width of 130-150 eV was detected in outburst (Oosterbroek et al. 1996). There is little other evidence for peculiarity of any abundances in V404 Cyg aside from a higher than expected lithium abundance in the companion (Casares et al. 1993, Casares & Charles 1994, Martin et al. 1992) which may be associated with the ADAF (Yi & Narayan 1997), although other Li production scenarios have also been proposed (e.g. Martin et al. 1992). The possible calcium line at 4.08 keV is intriguing, although this is not a secure detection. Ca-44

could be produced as a secondary decay product of Ti-44 (half life of ~ 86 years), which is produced in a supernova explosion (Theiling & Leising 2006), however this system's supernova could not have been recent enough for an overabundance to remain, and no overabundance is seen in the optical spectra. Other explanations for higher abundances of calcium have been proposed in the context of nucleosynthesis within thick accretion disks with very low viscosity (Arai & Hashimoto 1992, note Fig. 4; Mukhopadhyay & Chakrabarti 2000, Jin, Arnett & Chakrabarti 1989) but it would be premature to invoke such models without a more secure detection.

7. CONCLUSIONS

We have presented new *XMM-Newton* spectroscopy of the brightest quiescent stellar mass black hole, V404 Cyg. Fits to the continuum statistically reject all fitting models considered with the exception of power-law or bremsstrahlung emission. We place stringent new upper limits (52 eV, 90% confidence) on the presence of a narrow 6.4 keV line from neutral iron. Previous upper limits on the equivalent width of the 6.4 keV iron line emission were found to be ~ 800 eV (Kong et al. 2002), an improvement by a factor of 15. We also place a limit of 110 eV on ionized iron emission at 6.7 keV, roughly a factor of 2 below a specific model prediction.

Overall, our results are consistent with the common interpretation of the quiescent state involving a truncated accretion disk, within which a diffuse quasi-spherical

coronal/ADAF flow exists and attempts to cool itself by optically-thin emission. Variations like the adiabatic inflow/outflow (Blandford & Begelman 1999) allow for a significant fraction of the outer material to be lost to an outflow at large radii, and have rotation.

The lack of strong ionized lines apparently argues against a strong outflow/wind in the context of specific ADAF models considering winds (Narayan & Raymond 1999), where lower central accretion rates correspond to an enhancement on the bremsstrahlung emission and line widths. It is hard to draw strong general conclusions from this specific comparison, however. Indeed we know from radio observations that V404 Cyg does power a synchrotron emitting outflow (whether this comes from the innermost region or not is not known) (Gallo, Fender, & Hynes 2005).

This work is based on observations obtained with *XMM-Newton*, an ESA science mission with instruments and contributions directly funded by ESA Member States and NASA. The authors would like to thank Juhan Frank and Chris Mauche for their helpful comments. JC acknowledges support from the Spanish Ministry of Science and Technology through the project AYA2002-03570. We acknowledge support from the *XMM* Guest Observer Program and grant NNG06GB64G. CB acknowledges support from the LaSpace GSRA.

REFERENCES

- Arai, K., Hashimoto, M., 1992, *A&A*, 254, 191
 Arnaud, K.A., 1996, *Astronomical Data Analysis Software and Systems V*, eds. Jacoby G. and Barnes J., p17, ASP Conf. Series volume 101.
 Blandford, R.D., Begelman, M.C., 1999, *MNRAS*, 303, L1
 Campana, S., Parmar, A.N., Stella, L., 2001, *A&A*, 372, 241
 Campana, S., Stella, L., Belloni, T., et al., 2002, *A&A*, 384, 163
 Casares, J., & Charles, P.A. 1994, *MNRAS*, 271, L5
 Casares, J., Charles, P.A., Naylor, T., 1992, *Nature*, 355, 614
 Cash, W. 1979, *ApJ*, 228, 939
 Churazov, E., Gilfanov, M., Forman, W., Jones, C., 1996, *ApJ* 471, 673
 Fabian, A.C., Miniutti, G., 2005, in Wiltshire, D.L., Visser, M., Scott, S.M., eds, *Kerr Spacetime: Rotating Black Holes in General Relativity*. Cambridge University Press, Cambridge, in press (astro-ph/0507409)
 Fender, R.P., Gallo, E., Jonker, P.G., 2003, *MNRAS*, 343, L99
 Gallo, E., Fender, R.P., Hynes, R.I., 2005, *MNRAS*, 356, 1017G
 Garcia, M.R., McClintock, J.E., Narayan, R., Callanan, P., Barret, D., & Murray, S.S., 2001, 553, L47
 George, I.M., Fabian, A.C., 1991, *MNRAS*, 249, 352
 Gierlinski, M., Zdziarski, A.A., Done, C., et al. 1997, *MNRAS*, 288, 958
 House, L.L., 1969, *ApJS*, 18, 21
 Hynes, R.I., 2005, ASP Conf. Ser. 330: *The Astrophysics of Cataclysmic Variables and Related Objects*, 330, 237
 Hynes et al 2006 in prep
 Hynes, R.I., Charles, P.A., Garcia, M.R., et al., 2004, *ApJ*, 611, 125
 In 't Zand, J.J.M., Markwardt, C.B., Bazzano, A., et al., 2002, *A&A*, 390, 597
 Jin, L., Arnett, W.D., Chakrabarti, S.K., 1989, *ApJ*, 336, 572
 Kong, A.K., McClintock, J.E., Garcia, M.R., Murray, S.S., Barret, D., 2002, *ApJ*, 570, 277
 Makino, F., Wagner, R.M., Starrfield, S., Buie, M.W., Bond, H.E., Johnson, J., Harrison, T., Gehrz, R.D., 1989 *IAUC*, 4786
 Makishima, K., 1986, *LNP*, 266, 249
 Malzac, J., Merloni, A., and Fabian, A.C., 2004, *MNRAS*, 351, 253
 Martin, E.L., Rebolo, R., Casares, J., Charles, P.A., 1992, *Nature*, 358, 129
 Matt, G., Fabian, A.C., Ross, R.R., 1996, *MNRAS*, 278, 1111
 Matt, G., Fabian, A.C., Ross, R.R., 1993, *MNRAS*, 262, 179
 Martocchia, A., Matt, G., Karas, V., Belloni, T., Feroci, M., 2002, *A&A*, 387, 215
 Miller, J.M., Fabian, A.C., Wijnands, R., et al., 2002, *ApJ*, 570, 69
 Miller, J.M., 2006, *A Short Review of Relativistic Iron Lines from Stellar-Mass Black Holes*, astro-ph/0609447
 Mukhopadhyay, B., Chakrabarti, S.K., 2000, *MNRAS*, 313, 1029
 Narayan, R., Barret, D., & McClintock, J.E. 1997a, *ApJ*, 482, 448
 Narayan, R., Garcia, M., McClintock, J.E., 2002, in *Grzadyan V., Jantzen R., Ruffini R., eds, Proc. IX Marcel Grossmann Meeting*. World Scientific, Singapore, 405
 Narayan, R., & Raymond, J. 1999, *ApJ*, 515, L69
 Oosterbroek, T., Parmar, A.N., Sidoli, L., in't Zand, J.J.M., Heise, J., 2001, *A&A*, 376, 532
 Oosterbroek, T., van der Klis, M., Vaughan, B., et al., 1996, *A&A*, 309, 781
 Raymond, J.C., Smith, B.W., 1977, *ApJS*, 35, 419
 Remillard, R.A., McClintock, J.E., 2006, *ARA&A*, 44, 49
 Shahbaz, T., Ringwald, F.A., Bunn, J.C., Naylor, T., Charles, P.A., Casares, J., 1994 *MNRAS*, 271, L10
 Theiling, M.F., Leising, M.D., 2006, *NewAR*, 50, 544T
 Quataert, E., & Narayan, R. 1999, *ApJ*, 520, 298
 Wagner, R.M., Starrfield, S.G., Hjellming, R.M., Howell, S.B., Kreidl, T.J., 1994, *ApJ*, 429, L25
 Yuan, F., Cui, W., and Narayan, R., 2005, *ApJ*, 620, 905